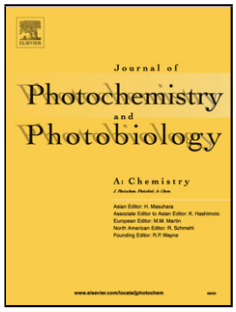

Title: Substitution of PPh_3^+ as a lipophilic cation on new water-soluble Co(II) and Zn(II) Schiff base complexes: effect of central metal and substitutional group of ligand on DNA-complex interaction

Authors: Zahra Asadi, Elahe Haddadi, Moslem Sedaghat

PII: S1010-6030(16)31088-7
DOI: http://dx.doi.org/doi:10.1016/j.jphotochem.2017.01.022
Reference: JPC 10511

To appear in: *Journal of Photochemistry and Photobiology A: Chemistry*

Received date: 18-11-2016
Revised date: 14-1-2017
Accepted date: 17-1-2017

Please cite this article as: Zahra Asadi, Elahe Haddadi, Moslem Sedaghat, Substitution of PPh3+ as a lipophilic cation on new water-soluble Co(II) and Zn(II) Schiff base complexes: effect of central metal and substitutional group of ligand on DNA-complex interaction, Journal of Photochemistry and Photobiology A: Chemistry http://dx.doi.org/10.1016/j.jphotochem.2017.01.022

Substitution of PPh_3^+ as a lipophilic cation on new water-soluble Co(II) and Zn(II) Schiff base complexes: effect of central metal and substitutional group of ligand on DNA-complex interaction

Zahra Asadi*, Elahe Haddadi, Moslem Sedaghat

Department of Chemistry, College of Sciences, Shiraz University, Shiraz 71454, Iran

* Corresponding author. E-mail address: zasadi@shirazu.ac.ir

Tel: +98 713 6137118; Fax: +98 713 646 0788

Graphical abstract

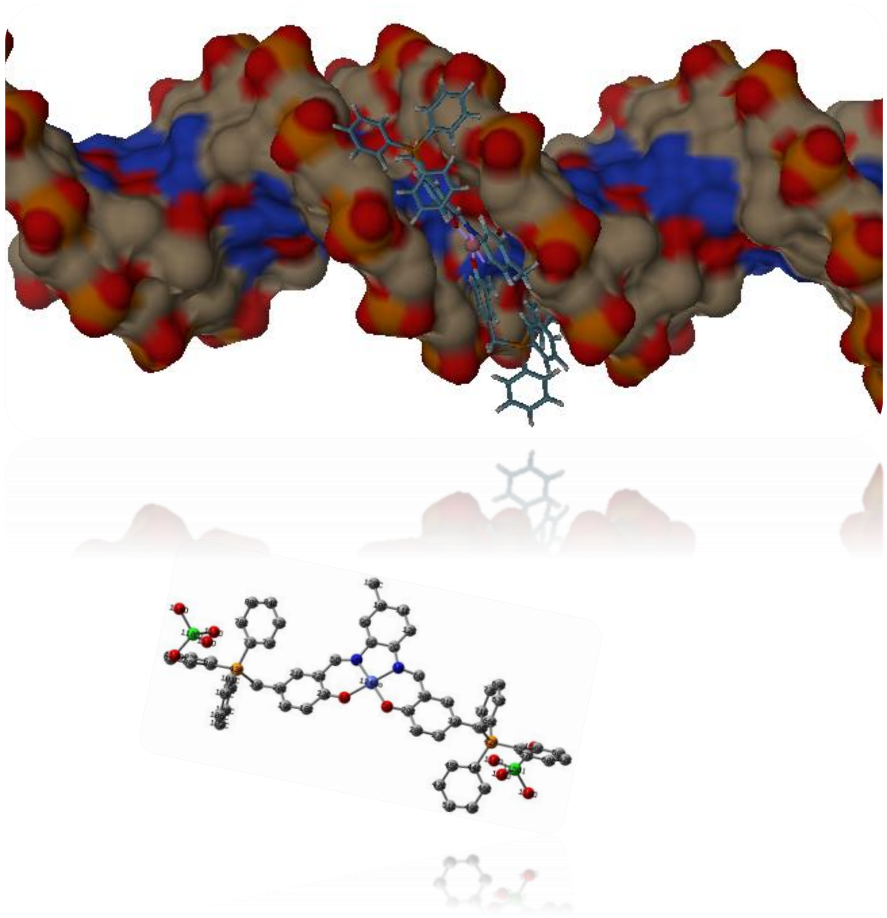

Highlights

- New series of water soluble complexes were synthesized and characterized.
- DNA binding potency of these complexes was investigated with different methods.
- Cytotoxicity of these complexes against Raji, Jurkat and A549 cell lines were studied.
- Docking studies were performed to further investigate the DNA binding interactions

Abstract

New series of water soluble Schiff base complexes by conjugating the lipophilic triphenylphosphonium cation to aromatic moiety of Schiff base ligand, aiming to increase the water solubility and passing through cell membrane were synthesized and characterized. Four new complexes; [N,N′-bis{5-[(triphenylphosphoniumchloride)-methyl]salicylidine}-phenylenediamine] with the formula [Zn(5-CH_2PPh_3-4-H-1,2-salphen)] $(ClO_4)_2$ (**1),** [Zn(5-

CH_2PPh_3-4-CH_3-1,2-salphen)]$(ClO_4)_2$ (**2),** [Zn(5-CH_2PPh_3-4-Cl-1,2-salphen)]$(ClO_4)_2$ (**3),** [Co(5-CH_2PPh_3-4-CH_3-1,2-salphen)]$(ClO_4)_2$ (**4)** were characterized by elemental analysis, FT-IR, ^{1}H NMR, ^{13}C NMR, ^{31}P NMR and UV-vis spectroscopy. Cobalt(II) complex also characterized by thermal gravimetry analysis (TG). DNA interaction studies were investigated by UV-vis absorption spectroscopy, viscosity measurements, circular dichroism (CD) spectroscopy and fluorescence spectroscopy. The DNA binding affinity (K_b) obtained from absorption spectroscopy had this order: **2**>**3**>**4**>**1>ligand(L)** which revealed that metal complexes had more propensities to interact with DNA. In comparing the metal complexes; Zn(II) complexes revealed DNA binding stronger than the corresponding Co(II) analogue. All the complexes displayed cytotoxicity against Raji, Jurkat and A549 cell lines with potency more than that of *cisplatin* and thus they are good candidate to act as promising anticancer drug. Finally, docking studies were performed to further investigate the DNA binding interactions.

Keywords: water soluble, Schiff base complex, DNA, DFT, docking study, anticancer activity.

1. Introduction

Transition metal Schiff base complexes are important compounds due to their structural similarities with natural biological molecules, like vitamin B_{12}[1] and they have biological activities including antifungal, antibacterial, anticancer and herbicidal applications[2-14]. Such inorganic compounds prepare wide field for the design of metal based drugs. Among transition metals, the first row transition metals have attracted special attention. Studies on their DNA binding affinity and other biological activities have been done during recent years[15-17]. The reasons of this attention are directly related to the coordination and redox properties of transition metal compounds[18]. To design effective anticancer drugs, it is essential to assess the interactions of metal complexes with DNA[19]. These kinds of studies are also important to understand the toxicity of drugs [20-23].

Complexes bind to DNA via covalent and non-covalent interactions. *Cisplatin*; an important anticancer drug; bind to DNA through covalent interaction but this kind of interaction has significant side effects because of the formation of covalent cross-links. Drugs that interact

through non-covalent modes are of great importance, this mode of binding contains electrostatic interaction, groove binding and intercalation. Intercalation of drugs is related to the type of metal and ligand[24]. Metal complexes with aromatic ligands intercalate between DNA base pairs through the π-π interaction of the aromatic section with the stacked aromatic planes of the nitrogen bases. Cationic molecules have electrostatic interactions with the negatively charged phosphate groups of DNA. In groove binding, hydrogen bonding of metal complexes with oxygen and /or nitrogen atoms of the DNA bases or with the sugar fragments, plays an important role in interaction[25].

Transition metal compounds are of great interest as potential drugs because they are essential for the normal functioning of living organisms. In many researches, zinc(II) complexes showed biological activity such as antimicrobial efficacy, antibacterial and DNA interaction[26-29]. For studying the biological activity of the metal complexes, it is important to select a green solvent for example H_2O, and provide natural biological condition. Most of the metal Schiff base complexes are not soluble in water but with providing some ionic groups on the Schiff base ligand the hydrophilicity of the complex can be increased. Recently, Murphy and Smith published a review on mitochondria-targeted antioxidants which developed by conjugating the lipophilic triphenylphosphonium cation which placed on an antioxidant moiety[30]. The main characteristics of these compounds are their ability to pass easily through all biological membranes.

In recent years, we have studied the interaction of some water soluble metal Schiff base complexes with human serum albumin (HSA)[31] and bovine serum albumin (BSA)[32-34]. In this paper, the interaction of some zinc(II) and cobalt(II) water soluble Schiff base complexes with Herring Sperm DNA (HS-DNA) was studied. The zinc(II) complexes possessed different substitutional groups on the amine bridge of the Schiff base (Scheme 1). The final product, $[M(5\text{-}CH_2PPh_3\text{-}4\text{-}R\text{-}1,2\text{-salphen})](ClO_4)_2$ (M=Zn, R=H (**1),** M=Zn, R=CH_3 (**2),** M=Zn, R=Cl (**3),** M=Co, R=CH_3 (**4),** and the free ligand were fully characterized by various physicochemical techniques, namely, elemental analyses and spectral (FT-IR, ^{1}HNMR, ^{13}CNMR, ^{31}PNMR, UV-vis). The binding property of the complexes and ligand with HS-DNA under physiological conditions was studied using UV-vis spectrophotometry, DNA viscosity measurements, fluorescence spectroscopy and circular dichroism (CD) spectroscopy. Also the anticancer activities of the complexes and molecular docking studies were performed. The main goal of this

study is investigation of the structural features on the DNA binding interactions. Two important factors in the interaction of complexes with DNA (external binding and π–π stacking) were considered in the designing of complexes by putting $CH_2PPh_3^+$ substituent on the aromatic moiety of the Schiff base ligand. These groups also increased the water solubility of the complexes and their easily passing through all biological membrane.

2. Experimental

2.1. Reagents and instruments

All chemicals were purchased commercially. Experiments were performed in Tris-HCl buffer at pH 7.2. Stock solution of FS-DNA was prepared by dissolving approximately 1-2 mg of FS-DNA in 2 mL Tris-HCl buffer and stored for 24h at 4°C. The concentration of HS-DNA solution was determined by spectrophotometry at 260 nm using an extinction coefficient (ε) of 6600 $M^{-1}cm^{-1}$. DNA solutions were used no more than 4 days. A solution of FS-DNA in the buffer gave a ratio of UV absorbance at 260 and 280 nm of 1.98, indicating that the DNA was sufficiently free from protein[35]. The ^{1}HNMR and ^{13}CNMR spectra were recorded on Bruker Avance DPX 250MHz spectrometer. ^{31}PNMR spectra were recorded on Bruker Ultrashield 400MHz spectrometer. Elemental analysis for C, H and N were carried out by Thermo Fininngan-Flash 1200. FT-IR spectra were recorded as KBr pellets on a Shimadzu FTIR 8300 infrared spectrophotometer in the range of 4000–400cm^{-1}. Perkin–Elmer (LAMBDA 2) UV-vis. spectrophotometer was used to measure the UV-vis. spectra and Perkin-Elmer (LS45) spectrofluorimeter equipped with a Lauda-ecoline-RE 104 thermostat for emission spectra. Thermal gravimetric analyses were recorded on a Perkin-Elmer Pyris Diamond model. Circular dichroism spectra of DNA were obtained by using Aviv Model 215 spectropolarimetre equipped with a peltier temperature control device.

2.2. Synthesis

2.2.1. Synthesis of (3-formyl-4-hydroxybenzyl)triphenylphosphoniumchloride

A mixture of salicylaldehyde (0.08mol), para-formaldehyde (0.05mol) and 50mL of conc. HCl was stirred at room temperature for 48h. The resulting dark red powder precipitate was collected by filtration, washed with 0.5% $NaHCO_3$ solution then water, and dried in vacuum. The product was crystallized from acetonitrile and petroleum ether. A mixture of 5-

chloromethylsalicylaldehyde (0.06mol) and triphenylphosphine (0.06mol) in 200mL acetonitrile was refluxed for 8h and cooled. The precipitated phosphonium salt was filtered off and washed with ether.

Yield: 41%, m.p.=250-251°C, Color: white, Anal. Found(Calc.):$C_{26}H_{22}PO_2Cl$: C, 72.27(72.14); H, 5.14 (5.12). FT-IR (KBr, cm^{-1}): 3741(ν_{OH}), 2869(ν_{C-H}), 1674($\nu_{C=O}$). ^{1}H NMR (250 MHz, DMSO-d_6): δ (ppm) = 11.18 (s, 1H, OH),10.14 (s, 1H, CHO), 7.87 (dd, *J* = 10.1, 4.5 Hz, 3H, ArH), 7.69 (dq, *J* = 12.5, 7.6 Hz, 12H, ArH), 7.26 – 7.15 (m, 1H, ArH), 7.11– 6.92 (m, 2H, ArH), 5.13 (d, *J* = 15.0 Hz, 2H, CH_2). (spectral data in Fig.S1)

Synthesis of [N,N′-bis{5-[(triphenylphosphoniumchloride)-methyl]salicylidine}-phenylenediamine] (L)

To a vigorously stirred solution of (3-formyl-4-hydroxybenzyl)triphenylphosphonium chloride (1.25mmol) in 50 mL water, an ethanolic solution (20 mL) of pheneylenediamin (0.62 mmol) was added dropwisely. The solution turned to light yellow and the mixture refluxed for 3 h. After that, $NaClO_4$ (1.25 mmol) dissolved in a minimum amount of water (5 mL) and was added. The resulting yellow powder (Scheme 1) was collected by filtration, washed with cold ethanol and ether and dried in the air.

Yield: 85%. m.p (>310°C), Color: light yellow. Anal. Found (Calc.) for $C_{58}H_{48}Cl_2N_2O_{10}P_2$: C, 65.55 (65.36); H, 4.57 (4.54); N, 2.50 (2.63). FT-IR (KBr, cm^{-1}): 1650 ($\nu_{C=N}$), 1487 ($\nu_{C=C}$), 1087, 650 (ν_{ClO4}-). ^{1}HNMR (250 MHz, DMSO-d_6) δ (ppm): 11.12 (s, 2H, OH), 8.53(s, 2H, HC=N), 7.87- 6.82 (m, 40H, ArH) 5.06 (dd, *J* = 15.1, 3.1Hz, 4H, CH_2P). ^{13}C NMR (250 MHz, DMSO-d_6) δ (ppm): 160.9, 160.8 (C=N), 138.0, 137.9, 135.0, 134.0, 133.9, 131.5, 130.4, 130.1, 129.9, 128.8, 122.4, 118.2, 118.0, 117.95, 116.9 (aromatic carbons), 34.2, 33.9 (CH_2). ^{31}P NMR (400 MHz, DMSO-d_6) δ (ppm): 22.58. UV–vis. (H_2O): λ_{max} (nm) = 387, 333. (spectral data in Figs. S2, S3, S4).

2.2.2. Synthesis of the complexes

To a vigorously stirred solution of (3-formyl-4-hydroxybenzyl)triphenylphosphonium chloride (1.25mmol) in 50mL water, metal(II) acetate (0.62mmol) dissolved in water (l0mL) was added. Then an ethanolic solution (20mL) of diamine (0.62 mmol) was added dropwisely to synthesize the complexes. The solution turned to yellow and the mixture refluxed for 3h. After

that, $NaClO_4$ (1.25mmol) was dissolved in a minimum amount of water and added to the reaction mixture. The resulting yellow powder was collected by filtration, washed with cold ethanol and ether and dried in the air. All steps in synthesis of Co(II) complex were done under N_2 atmosphere.

a)[N,N′-bis{5-[(triphenylphosphoniumchloride)-methyl]salicylidine}-phenylenediaminato] zinc(II)perchlorate (**1**), Yield: 75%, Color: Yellow, m.p.>250°C, Anal. Found (Calc.) for $C_{58}H_{46}Cl_2N_2O_{10}P_2Zn.H_2O$: C, 60.55 (60.78); H, 4.17 (4.13); N, 2.40 (2.44). FT-IR (KBr, cm^{-1}): 3440(ν_{O-H}), 1620($\nu_{C=N}$), 1527($\nu_{C=C}$), 1103, 686(ν_{ClO4}), 617 (ν_{M-N}), 493(ν_{M-O}).^{1}H NMR (250 MHz, DMSO-d_6) δ (ppm) = 6.41-7.86 (m, 40H, ArH), 8.52 (d, 2H, HC=N), 4.90 (d, 4H,CH_2P). ^{13}C NMR (250 MHz, DMSO-d_6) δ (ppm): 162.1, 161.3 (C=N), 157.7, 149.7, 146.6, 144.7, 137.5, 135.0, 134.8, 134.0, 133.9, 130.2, 130.0, 129.6, 123.6, 123.2, 118.5, 117.7, 116.1, 113.7 (aromatic carbons), 34.6, 34.2 (CH_2). ^{31}P NMR (400 MHz, DMSO-d_6) δ (ppm): P_a (21.77), $P_{a'}$ (21.69). UV-vis.(H_2O): λ_{max}(nm) = 382, 268. (spectral data in Figs.S2, S3, S4)

b)[N,N′-bis{5-[(triphenylphosphoniumchloride)-methyl]salicylidine}-4-methyl-phenylene diaminato]zinc(II)perchlorate (**2**). Yield: 88%; m.p. >250°C, Color: Yellow, Anal. Found (Calc.): $C_{59}H_{48}Cl_2N_2O_{10}P_2Zn.H_2O$: C, 61.14 (61.02); H, 4.36 (4.34); N, 2.43 (2.41). FT-IR (KBr, cm^{-1}): 3463(ν_{O-H}), 1620($\nu_{C=N}$), 1473($\nu_{C=C}$), 1095, 694(ν_{ClO4}), 624(ν_{M-O}), 493(ν_{M-N}). ^{1}H NMR (250 MHz, DMSO-d_6) δ (ppm) = 8.51(s, 1H, HC=N), 8.47(s, 1H, HC=N), 6.40-7.87 (m, 41H, ArH), 4.93 (d, 4H, CH_2P), 2.37 (s, 3H, CH_3). ^{13}C NMR (250 MHz, DMSO-d_6) δ (ppm): 162.4, 161.6(C=N), 155.7, 150.5, 146.2, 142.2, 140.3, 139.5, 138.7, 135.0, 134.0, 133.9, 130.2, 130.0, 126.8, 126.0, 122.4, 122.0, 118.5, 117.3, 10.4.6 (aromatic carbons), 34.9, 34.1 (CH_2), 30.2 (CH_3). ^{31}P NMR (400 MHz, DMSO-d_6) δ (ppm): P_a (21.90), $P_{a'}$ (21.75). UV-vis. (H_2O): λ_{max}(nm) = 460, 268. (spectral data in Figs. S2, S3, S4)

c)[N,N′-bis{5-[(triphenylphosphoniumchloride)-methyl]salicylidine}-4-chloro-phenylene diaminato]zinc(II)perchlorate (**3**), Yield: 61%, m.p>250°C, Color: Yellow, Anal. Found (Calc.):$C_{58}H_{45}Cl_3N_2O_{10}P_2Zn$: C,59.62(59.86); H,3.81(3.90); N, 2.50(2.41). FT-IR (KBr, cm^{-1}): 3440 (ν_{O-H}), 1612 ($\nu_{C=N}$), 1488 ($\nu_{C=C}$), 1110, 686 (ν_{ClO4^-}), 624 (ν_{M-N}), 493 (ν_{M-O}), ^{1}H NMR (250 MHz, DMSO-d_6, room temperature) δ(ppm) =8.51 (d, 2H, HC=N), 6.54-7.19(m, 41H, ArH),

4.95(d, 4H,CH_2P). ^{13}C NMR (250MHz, DMSO-d_6) δ (ppm): 162.7, 161.5 (C=N), 155.2, 150.2, 146.3, 142.5, 140.7, 139.0, 138.0, 135.7, 134.2, 133.0, 130.8, 130.0, 126.4, 126.0, 122.5, 122.3, 118.0, 117.0, 104.5 (aromatic carbons), 34.8, 34.6 (CH_2). ^{31}P NMR (400 MHz, DMSO-d6) δ (ppm): P_a (21.95), $P_{a'}$ (21.80). UV-vis. (H_2O): λ_{max}(nm) =380, 265. (spectral data in Figs.S2,S3,S4)

d)[N,N′-bis{5-[(triphenylphosphoniumchloride)-methyl]salicylidine}-4-methyl-phenylene diaminato]cobalt(II) perchlorate (**4**), Yield: 64%, m.p >250°C, Color: Brown, Anal. Found (Calc.): $C_{59}H_{48}Cl_2N_2O_{10}P_2Co.H_2O$: C, 61.49(61.36); H, 4.29(4.36); N, 2.51(2.43), FT-IR (KBr, cm^{-1}): 3448(ν_{O-H}), 1612($\nu_{C=N}$), 1488($\nu_{C=C}$), 1095, 709(ν_{ClO4^-}), 624(ν_{M-N}), 501(ν_{M-O}). UV-vis. (H_2O): λ_{max}(nm) = 464, 265. TG/DTG: mass loss percent %, Found (Calc.) : H_2O: 2 (1.5) , $2ClO_4$: 21(20.4). (spectral data in Figs. S3, S4, S5)

***CAUTION**! The perchlorate salts could be potentially explosive. Therefore, only small quantities of the sample were handled to avoid any possible explosion.*

Solubility and stability

All the synthesized complexes were soluble in water, dimethylformamide (DMF) and dimethylsulfoxide (DMSO). The complexes were stable in the solid phase at ambient temperature in the light. The solutions were stable for a long period in light and were not air sensitive.

2.3. DNA binding experiments

Absorption titration experiments were conducted by keeping the concentration of the compounds at 50μM while varying the concentration of DNA from 0 to 260 μM. Absorption values were recorded after each successive addition of DNA solution, followed by an equilibration period. Fluorescence measurements of the metal complex at an excitation wavelength of 320 nm, and emission spectra between 340-550 nm were recorded. Each spectrum was recorded at 200nm/min scan speed and 10nm slit width for both the excitation and emission monochromators. Fluorescence measurements were carried out by keeping the concentration of

the complexes at 30μM while varying the DNA concentration from 0 to 260 μM. Viscosity measurement was performed by using an Ostwald viscometer, immersed in a thermostated water-bath maintained to 25.0 ± 0.1°C. The DNA concentration was fixed at 10μM, and flow time was measured with a digital stopwatch. The measurements were carried out three times for each sample for calculating the average flow time. The plots of relative specific viscosity $(\eta/\eta_o)^{1/3}$ (where η_o and η are the specific viscosity contributions of DNA in the absence (η_o) and in the presence of the complex (η)) were drown against r_i (r_i=[complex]/[DNA]= 0, 0.05, 0.10, 0.15, 0.20, 0.23).

Circular dichroism spectrum of DNA was obtained by using JASCO J-716 spectropolarimeter equipped with a peltier temperature control device. All experiments were done using a 1 or 0.2 cm path quartz cell. Each CD spectrum was collected after aveRajing over at least 2 accumulations using a scan speed of 100nmmin^{-1} and a 1s response time. Machine plus cuvette baselines were subtracted and the resultant spectrum zeroed outside the absorption bands.

2.4. Computational details

The structure of complexes was optimized with density functional theory (DFT) by B3LYP method and 6-311g basis set for all atoms. In this work we used gauss view 05 for drawing the structure of these complexes and Gaussian 03 program to ground state geometry optimization and other calculations.

2.5. Molecular docking

The molecular geometry of complexes was subjected to energy minimization by DFT calculations at the B3LYP method and 6-311G basis set for all atoms.

The crystal structure of DNA (PDB code: 4HC9) was taken from the protein Data bank (www.rsbs.org/pdb)[36]. Which had been equilibrated at a nuclei-like condition was used as the receptor. Then, the optimized compounds were imported to Molegro Virtual Docker (MVD)[37] to carry out the docking simulations. This software generates the best DNA-ligand configurations according to several scoring criteria such as Moldock and Rerank scores. In MVD the units are arbitrary, but an ideal hydrogen bond contributes to the overall energy[38]. We have selected score as Moldock score [GRID], with GRID resolution of 0.3 Å. Algorithm selected for docking was Moldock along with number of runs as 20 [39]. For each docking calculation, 10 different poses were done.

2.6. Cell culture and MTT assay for analysis of anti-cancer properties of the complexes

The growth inhibitory effects of the complexes against three cell lines including Jurkat human T cell leukemia, Raji Burkitt's lymphoma and A549 lung carcinoma were examined by 3-(4,5-dimethylthiazol-2-yl)-2,5-diphenyltetrazoliumbromide (MTT) assay. The cell lines were cultured in RPMI 1640 medium (Sigma, St. Louis, MO) supplemented with 10% fetal calf serum (Gibco, Berlin, Germany). Cells were maintained at 37ºC with 5% CO_2 and 95% humidity. The cells were fed until confluent and expanded by trypsinization (for A549), then subcultured at lower numbers in new culture flasks. A predetermined number of cells (15×10^3 for Jurkat and Raji cells and 7.5×10^3 for A549 cells) were seeded in the wells of a 96-well plate with varying concentrations of the complexes (0.1–100 μg/mL) and incubated at 37ºC with 5% CO_2 for 48 h. Cells treated only with dimethylsulfoxide (solvent) at a concentration equal to the test wells was used as negative control and those treated only with
cisplatin as positive control. 10 μL MTT solutions (5mg mL^{-1} in RPMI medium) were added to each well and incubation was continued for 4 h. At the end, the produced insoluble formazan was dissolved by adding DMSO and shaking for 10 min. Then, the optical density (OD) was read at 570nm with a reference wavelength of 630 nm in a microplate reader (Bio-Tek's ELx808, VT). The percentage of growth inhibition was determined as follows; [1–(test OD/negative control OD)] × 100. The concentration of 50% cell inhibition (IC_{50}) value was calculated from the graph of inhibition percentage against different compounds concentrations.

3. Results and discussion

3.1. Spectral properties of the complexes

The ligands and complexes 1-4 were isolated using the procedure reported (Scheme 1). All the complexes were characterized by elemental analysis, FT-IR, ^{1}H NMR, ^{13}C NMR, ^{31}P NMR, UV–vis. Spectroscopy. In the ^{1}H NMR spectrum of the precursor aldehyde a single signal at 11.60 ppm was assigned to OH proton. Aldehydic proton was revealed at 10.63ppm and the aromatic protons were revealed in the range 7.41-8.37 ppm. In the spectra of the ligand, the singlet signal at 11.09 ppm is assigned to the OH group. However, in the spectra of the complexes there was no resonance attributable to OH, indicating the coordination of ligand in the anionic form upon deprotonation. In the spectrum of symmetrical complex **1** a single signal was observed for the -C(H)=N proton[40, 41] which clearly indicated that the magnetic environment

was equivalent for the imine protons. But in the ^{1}H NMR spectra of the unsymmetrical complexes **2**, **3** two imine protons were revealed due to different chemical environments. Signals due to OH of the aldehyde were absent in the spectra of the complexes revealing the deprotonation of OH groups and coordination through the oxygen atoms[42]. The doublet at about 4.90 ppm was associated to the CH_2 group. ^{1}H NMR spectrum of the cobalt(II) complex gave no signal due to its paramagnetism.

In the ^{13}C NMR spectra, resonances observed around 160.0 - 163.0 ppm were due to the azomethine carbons and aromatic carbon atoms observed around 103.0 - 157.0 ppm. The CH_2 carbon resonance is observed around 34.0 ppm.

^{31}P NMR spectra were recorded to confirm the presence of triphenylphosphine. One or two peaks observed at 20.0-23.0 ppm suggested the presence of two equivalent or non-equivalent triphenylphosphines.

In the FT-IR spectrum of the aldehyde a broad medium intensity band at 3741cm^{-1} was assigned to O-H vibration and medium-weak band at 1674cm^{-1} to the CHO vibration. The presence of strong imine (C=N) bands at 1634cm^{-1} (**L**), 1620cm^{-1} (**1,2**) and 1612cm^{-1} (**3,4**) confirmed the formation of the Schiff base ligand and Schiff base complexes. C=N vibration frequency of **1** shifts toward lower frequencies in comparing with the ligand. This suggested the coordination of ligand to metal ion through the nitrogen of azomethine which resulted in decreasing the bond order of (C=N) linkage. Two peaks around 1110 and 700cm^{-1} were assigned to the ClO_4 groups. The vibration bands around 3440cm^{-1} was due to the presence of lattice and coordinated water in the complexes[43]. In the lower frequency region medium-weak bands at around 620 and 493cm^{-1} were assigned to (M–N) and (M–O) vibrations, respectively.

In the UV-vis absorption spectra of the compounds, the intensive absorption bands at 260-464 nm were assigned to the $\pi \rightarrow \pi^*$ and $n \rightarrow \pi^*$ transitions of aromatic rings or azomethine groups of the Schiff base.

The thermal decomposition of the complex **4** was studied to evaluate its thermal stability. During the thermal analysis, heating rates were set to 20ºCmin^{-1} under nitrogen atmosphere, and the weight loss was measured from the ambient temperature up to 800ºC. This method was also used to establish that only one water molecule was coordinated to the central metal and the water molecule did not coordinate strongly and was removed easier than the tetradentate ligand. Complex **4** decomposed in three steps. The first step was related to dehydration that occurred

between 240-280°C. Dehydration process was associated with exothermic DTA peak. The second step, which occurred in the range 280-350°C, was related to the release of both ClO_4 groups. The pyrolysis of remained part of the ligand took place as shown by an exothermic DTA peak in the range 350-800°C. (Fig.S5).

3.2. DNA binding studies

3.2.1. Absorption spectral studies

Generally, determination of the binding strength and the mode of DNA binding with small molecules is done by using electronic absorption spectroscopy [44]. Two important evidences in this method are: the change in absorbance and shift in wavelength upon addition of increasing concentrations of DNA solution in a fixed concentration of metal complexes. These evidences give valuable information on the mode of interaction. Hypochromism with or without a small red or blue shift guides to intercalation mode of binding. The intercalative mode involves a strong stacking interaction between the planar aromatic chromophore and the base pairs of DNA[45, 46]. The extent of hypochromism is commonly consistent with the strength of the intercalative binding interaction[47-50].

In studying the interactions of the synthesized complexes, one of the important modes of interactions was electrostatic attraction between the two positively charged residues of the metal complexes (PPh_3^+) and negatively charged phosphate groups of DNA. Also phenyl groups of complexes can interact with DNA through intercalation.

The absorption spectra of the complexes in the absence and presence of FS-DNA are shown in Fig. 1 and Fig. S6. It was observed that by addition of HS-DNA, the intensity of the absorption band at around 300-420 nm was reduced (hypochromism) with no shift. Hypochromism indicated the intercalative binding of the complexes between DNA duplex[51, 52]. In the intercalative binding mode, the π^* orbital of the intercalated complex could interact with the π orbital of the DNA base pairs, thus, the $\pi \rightarrow \pi^*$ transition energy was decreased and the coupling π orbital partially filled by electrons, so, decreasing the transition possibilities and concomitantly resulting in the hypochromism[53]. In order to obtain a more quantitative determination of the interaction strength, intrinsic-binding constant, K_b, was determined using equation (1)[54]:

$$[DNA]/(\varepsilon_a-\varepsilon_f) = [DNA]/(\varepsilon_b-\varepsilon_f) + 1/K_b(\varepsilon_b-\varepsilon_f) \qquad (1)$$

Where ε_a, ε_f and ε_b, are the apparent, free, and bound metal complex extinction coefficients, respectively. In particular, ε_f was determined by a calibration curve of the isolated metal complex in aqueous solution, following the Beer's law. ε_a was determined as the ratio between the measured absorbance and the complex concentration, A_{obs}/[complex].

A plot of [DNA]/(ε_b-ε_f) versus [DNA] gave a slope of 1/(ε_b-ε_f) and a Y intercept equal to 1/K_b(ε_b-ε_f); K_b is the ratio of the slope to the Y intercept.

Intrinsic binding constants for complexes **1-4** were in the $1.05\times10^4 M^{-1}$-$2.54\times10^2 M^{-1}$ range and for ligand (L) $1.22\times10^1 M^{-1}$. K_b for classical intercalators is in the order of 10^7 M^{-1}[53]. The values of intrinsic binding constants indicated the weaker intercalation of these complexes compared to classical intercalators.

By comparing the intrinsic binding constants of the complexes and ligand, it was found that Zn(II) complexes bound to DNA stronger than Co(II) complex and all the metal complexes stronger than free ligand (L). The order of binding affinity is **2**>**3**>**4**>**1**>**L**.

Effective nuclear charge for Zn atom is greater than Co atom. So it is concluded that Zn complexes had electrostatic interaction with DNA with more probability. From the UV spectroscopic titration, the main mode of binding was suggested to be intercalation.

The DNA binding affinity of **2** was stronger than **3** and **1**. Complex **2** contained methyl group on the bridged amine, so van der Waals interactions had a noticeable portion in binding mode, also hydrophobic interactions between the methyl groups in the complex and DNA interior was probable.

A halogen atom (Cl) as an electron withdrawing group on complex **3** makes it to be a more positive complex so the electrostatic portion of interaction increased. Complex **3** as a positively charged moiety was assumed to directly affect the negatively charged oxygen of the phosphate group of DNA. On the other hand organic halogen atoms are favorably involved in a wide variety of non-covalent biomolecules-complex interactions, such as halogen bonds C-X...O and hydrogen bonds C-X...H, so the affinity of **3** to interact with DNA increased.

In spite of the fact that effective charge of Zn atom is greater than Co atom but complex **4** containing methyl group on the ligand, so van der Waals interactions between methyl group and thymine methyl group of DNA and also hydrophobic interactions between the methyl groups and DNA interior, increased the binding affinity of **4** comparing to **1**[54].

However, the binding constants of complexes were much lower than the potential intercalators like ethidiumbromide ($7\times10^7 M^{-1}$)[55]. The K_b values (Table 1) were comparable to that of transition metal complexes[56-59].

3.2.2. Viscosity measurements

Hydrodynamic measurement that is sensitive to length change (i.e. viscosity) is considered as most critical test in predicting the nature of binding of the complexes to DNA. As in the intercalation mode of binding the complex is inserted between DNA base pairs, the length of DNA increases which leading to increase in DNA viscosity. In contrast bending (or kinking) of the DNA helix in the case of nonclassical intercalation, reduce the effective length of DNA and concomitantly its viscosity, while groove binding cause less pronounced changes (positive or negative) or no changes in DNA viscosity [55,60]. The values of relative specific viscosity $(\eta/\eta_0)^{1/3}$, here η and η_0 are the specific viscosity contributions of DNA in the absence and in the presence of the complex were plotted against r_i(r_i = [complex]/[DNA]) (Fig. 2). For **1-4 and L,** at lower concentration of the compound, the viscosity decreased or no changed and then increased at higher concentration of the compound. It is concluded that at least in the lower concentration of the complexes non classical intercalation (i.e. van der Waals interactions, groove binding or external binding) was main mode of binding although at higher concentration intercalation was the main mode of binding[54].

3.2.3. Fluorescence studies

A most commonly technique used to study the interaction between small molecules and DNA is fluorescence spectroscopy. One of the advantages of this technique is its high sensitivity and selectivity. Fluorescent spectroscopy can be used to determine the mode of binding of drugs to DNA. The effective intercalators cause a significant enhancement of the fluorescence intensity. But groove binding agents (agents that can have electrostatic, hydrogen bonding, or hydrophobic interactions) cause a decrease in fluorescence intensity because, after interaction, these agents are close to the sugar-phosphate backbone of DNA. Fluorescence emission is very sensitive to the

environment and spectral shifts (10-20nm) in the excitation and emission spectra have been observed during transferring the fluorophore between high and low polarity environment[60].

All synthesized complexes and ligand had emission spectra at room temperature thus binding to DNA can be study by titration of the compounds with various concentration of DNA. Figs.3, S7 show the emission spectra of the compounds in the absence and presence of HS-DNA.

For **1-4 and L** with increasing the concentration of DNA the intensity of emission spectra obviously decreased. Fluorescence quenching was described by the linear Stern-Volmer equation (2)[61]:

$$\frac{F_0}{F} = 1 + k_{SV}[Q] = 1 + k_q\tau_0[Q] \qquad (2)$$

where F and F_0 are the fluorescence intensities in the presence and the absence of quencher, respectively. K_{SV} is the Stern-Volmer quenching constant, [Q] is the total concentration of quencher, k_q was the bimolecular quenching constant, and τ_0 is the average lifetime of biomolecule in the absence of quencher, and its value is 10^{-8}s. Since fluorescence lifetime is naturally near 10^{-8}s, the bimolecular quenching constant (k_q) is calculated from $K_{sv}=k_q\tau_o$[61]. The fluorescence quenching curve of the complex by DNA (Fig.4) illustrates a good agreement with the linear curve of the Stern–Volmer equation and K_{sv} is calculated by the ratio of the slope to the intercept (Table 2). The moderately large value of K_{sv} indicated that the complexes **1-4** were bound to DNA. According to equation (2), k_q is greater than the limiting diffusion rate constant ($2.0\times10^{10}M^{-1}s^{-1}$) for a biomacromolecule, indicating the existence of a static quenching mechanism. In a static quenching mechanism, the fluorophore and the quencher form a complex in the ground state[62, 63].

To determine the strength of the interaction of complexes with DNA, the value of the binding constant (K_f) was resulted from a Scatchard equation (3)[64-67].

$$\log\left(\frac{F_0-F}{F}\right) = \log K_f + n\log[DNA] \qquad (3)$$

F_0 and F are the fluorescence intensities of the fluorophore in the absence and in the presence of different concentrations of DNA, respectively and n is the number of binding sites.

The values of K_f for **1-4** were found to be $3.68\times10^3M^{-1}$, $23.90\times10^3M^{-1}$, $3.78\times10^3M^{-1}$, and $4.16\times10^3M^{-1}$ and n=1.02, 1.25, 0.99, 1.1 respectively.

3.2.4. Anticancer studies

In the current study the synthetic Schiff base complexes were also screened for their anticancer activities on A549, Jurkat and Raji cell lines as the target. The cell lines were incubated in the presence of increasing concentrations of the complexes for 48 h, and then cytotoxicity was measured. Generally, all the compounds showed strong growth inhibitory activity against the cell lines. In order to compare the cytotoxic effects of the complexes, the IC_{50} values were determined. IC_{50} value is defined as the concentration of a compound where 50% of the cell growth is inhibited. As shown in Table 3, based on the IC_{50} values, the order of cytotoxic activity of complexes for A549 was **2** > **4** > **3** > **1**. The sequence of cytotoxic activity of complexes for Jurkat was **2**> **3**> **1**> **4** and for Raji cell line was **2**, **3**>**1**> **4**. As these results show complex **2** was more effective on A549 cells which are a solid tumor cell line (IC_{50}, 13.6 μg/mL). In contrast, complex **3** had a stronger activity against leukemia lymphoma cells (IC_{50},7.6 μg/mL for Jurkat and 9.1 μg/mL for Raji) compared to A549 (IC_{50}, 19.5 μg/mL). The IC_{50} values of *cis-platin* for A549 cell line was 79.4 μg/mL, 25.0 μg/mL for Jurkat and 30.1 μg/mL for Raji cells (Table 3).

3.3. DFT study

The geometries of complexes were optimized by using the GAUSSIAN 03 program. DFT calculations at the B3LYP method and 6-311G basis set for all atoms were done. The optimized geometries of the complexes are shown in Fig.5. Selected geometrical parameters including bond lengths, bond angles for all compounds are listed in Tables 4. Results showed that all of the bond lengths and bond angles are in the normal range.

According to data reported in Table 4, the water molecule was coordinated to the central metal of the complexes. Optimized structure suggested a square planar geometry around central atom with two "N" atoms from diamine and two "O" atoms of phenolic group. Therefore, axial position occupies by water molecule. Also results showed that two perchlorate groups bind to the complexes as ion pairs.

3.4. Docking investigations

The design of molecules that can recognize specific structures of nucleic acid play an important role to development of new chemotherapeutic drugs[68]. Molecular docking technique is a useful method to understand the drug-DNA interaction especially in the mechanistic study by

placing a small molecule in the binding site of DNA mainly in a non-covalent fashion.

The lowest-energy conformations show that all compounds occupied the minor grooves of DNA (Fig. 6 and Fig. S8). The ligands stretch inside the minor groove through the bridging phenyl group and the atoms surrounding it. By considering the ligand structure it is obvious that steric interactions played the dominant role in binding of the ligand to the DNA. The steric interactions arise from the (3-formyl-4-hydroxybenzyl) triphenylphosphonium chloride template and specifically its phenyl rings. From a detailed analysis of the docked structures, it appears that the metal complexes closed to the DNA structure from the metal center and oxygen groups of Schiff base ligand. Also it confirms the experimental finding that the nature of metal has high influence on interaction mode. By comparing the optimized structures of ligand and complexes, it is clear that the ligand is more folded than the complexes thus stretching of the complexes to the minor groove of DNA is more effective than the ligand.

The DNA binding affinity of the complexes may be predicted from the binding scores. The calculated binding scores for all optimized compounds are in the range of -96.953 – -114.267 (Table 5). It should be pointed out that the above docking calculations only allow a prediction to the binding affinity and the sterically acceptable conformations of the complexes to DNA.

The modes of binding of the complexes with DNA obtained from molecular docking studies correlate well with the experimental findings. Therefore, on the basis of Rerank Scores results, complex **2** has more DNA binding propensity as compared to the other complexes. The DNA binding affinity follows the order of: **2**>**3**>**4**>**1**>**L** as supported by the experimental findings. The results show that metal complexes act better than ligand and Zn complexes are better than Co complex in their interaction with DNA.

3.5. Circular dichroism spectroscopy

During the drug-DNA interactions the DNA morphology changes, a useful technique to monitor these changes is circular dichroism (CD), since CD signals are sensitive to small variations in the chiral conformation of DNA. The CD spectrum of free DNA is of the typical B-form, with a positive Cotton effect near 275 nm due to base stacking and a negative Cotton effect near 245 nm due to right-handed helicity[69] and these bands are quite sensitive to the mode of DNA interactions with small molecules. Thus simple groove binding and electrostatic interaction of small molecules display small or no perturbation on the base-stacking and helicity bands,

while the classical intercalation increases the base stacking and stabilizes helicity, and so enhances the intensity of the positive band[70]. Circular dichroism spectra were recorded at 25ºC with increasing amount of complexes (10μM to 40 μM) at constant concentration of the FS-DNA (200 μM). As shown in Fig. 7, by addition the complexes to the DNA solution a decrease in the intensity of positive band at 275nm was observed which confirm the interaction of complex with DNA through groove and/or surface bonding. Also, the decrease of the intensity of the positive band (275 nm) was likely to be because of a transition from the extended nucleic acid right-handed double helix to a more compact form[71] so the conformation of DNA had partly changed due to the binding interaction between these complexes and DNA. In the case of complex **2&3** (Fig. 7) a much larger decrease in intensity for the positive band at 275 nm and a new small positive band at 234 nm were observed. Since such a band and the shift of the main positive band toward shorter waves were characteristic of Z-DNA, it may mean that the DNA strands were locally converted into Z-DNA form[72] this showed that the DNA would interact with these complexes and might be distorted into other structures[73].

4. Conclusion

Some new Zn(II) and Co(II) Schiff base complexes have been synthesized and fully characterized. The DNA binding properties of complexes **1**–**4** and ligand (**L**) were examined by UV-vis absorption spectra, emission spectra, viscosity techniques and circular dichroism (CD). From these findings, it is concluded that, ligand had lower binding affinity than the complexes and groove binding was the main mode of interaction for complexes **1**-**4**. The binding of Zn(II) complexes are better relative to Co(II) complex that may be attributed either to the z* effect or geometry. Among the Zn(II) complexes: **2**>**3**>**1** and so complexes **2**&**3** containing CH_3 & Cl groups on the bridging ligand interacted strongly with DNA relative to complex **1,** because van der Waals interactions and hydrophobic interactions involve in the mode of interaction.

As easily passing through cell membrane is important in studying anticancer activity of the complexes

Moreover, the DNA docking studies revealed that the $-CH_2-PPh_3^+$ groups on the ligand play an important role in binding with the nucleotide phosphate unit of the DNA backbone and all the metal complexes (Zn, Co) interacted in the minor groove of DNA through the metal centre and oxygen groups of Schiff base ligand. The docking result also reveals the higher binding affinity

of complex **2** towards DNA receptors in comparison to complexes **1, 3, 4** and the free ligand.

The present study revealed that various metal effect and different Schiff base ligand on these complexes can influence the DNA binding events and *in vitro* anticancer activities, thus suggesting that the DNA binding ability and the anticancer activities may possibly be tuned through varying these factors in these compounds, which is useful for the design and synthesis of new metal-based drugs.

Acknowledgements

We are grateful to Shiraz University Research Council for its financial support.

References

[1] K.S. Prasad, L.S. Kumar, S. Chandan, R.N. Kumar, H.D. Revanasiddappa, Spectrochim. Acta. A 107 (2013) 108-116.
[2] K. Singh, M.S. Barwa, P. Tyagi, Eur. J. Med. Chem 41(1) (2006) 147-153.
[3] E. Gungor, S. Celen, D. Azaz, H. Kara, Spectrochim. Acta. A 94 (2012) 216-221.
[4] X.-B. Fu, G.-T. Weng, D.-D. Liu, X.-Y. Le, J. Photoch. Photobio. A 276 (2014) 83-95.
[5] A.A. Abu-Hussen, J. Coord. Chem 59(2) (2006) 157-176.
[6] M.S. Karthikeyan, D.J. Prasad, B. Poojary, K.S. Bhat, B.S. Holla, N.S. Kumari, Bioorg. med. chem 14(22) (2006) 7482-7489.
[7] S. Sathiyaraj, R.J. Butcher, C. Jayabalakrishnan, J. Mol. Struct 1030 (2012) 95-103.
[8] G. Ceyhan, C. Çelik, S. Uruş, İ. Demirtaş, M. Elmastaş, M. Tümer, Spectrochim. Acta. A 81(1) (2011) 184-198.
[9] J. Joseph, G.B. Janaki, J. Mol. Struct 1063 (2014) 160-169.
[10] Y.-T. Liu, G.-D. Lian, D.-W. Yin, B.-J. Su, Spectrochim. Acta. A 100 (2013) 131-137.
[11] S.A. Patil, S.N. Unki, A.D. Kulkarni, V.H. Naik, P.S. Badami, Spectrochim. Acta. A 79(5) (2011) 1128-1136.
[12] B.M. Kalshetty, S.S. Karabasannavar, R.S. Gani, M.B. Kalashetti, Drug invent. today 5(2) (2013) 105-112.
[13] B.S. Creaven, B. Duff, D.A. Egan, K. Kavanagh, G. Rosair, V.R. Thangella, M. Walsh, Inorg. Chim. Acta 363(14) (2010) 4048-4058.
[14] I. Babahan, F. Eyduran, E.P. Coban, N. Orhan, D. Kazar, H. Biyik, Spectrochim. Acta. A 121 (2014) 205-215.
[15] S. Sobha, R. Mahalakshmi, N. Raman, Spectrochim. Acta. A 92 (2012) 175-183.
[16] M. Sirajuddin, S. Ali, N.A. Shah, M.R. Khan, M.N. Tahir, Spectrochim. Acta. A 94 (2012) 134-142.
[17] N. Pravin, N. Raman, Inorg. chem. commun 36 (2013) 45-50.

[18] C. Rajarajeswari, R. Loganathan, M. Palaniandavar, E. Suresh, A. Riyasdeen, M.A. Akbarsha, Dalton Trans 42(23) (2013) 8347-8363.
[19] V. Uma, V. Vaidyanathan, B.U. Nair, B. chem. Soc. Jpn 78(5) (2005) 845-850.
[20] W. Szczepanik, J. Ciesiołka, J. Wrzesiński, J. Skała, M. Jeżowska-Bojczuk, Dalton Trans (8) (2003) 1488-1494.
[21] J.M. Woynarowski, A. Bartoszek, BBA-GENE. Struct. Expr 825(2) (1985) 244-253.
[22] T. Hatayama, M. Yukioka, BBA-GENE. Struct. Expr 740(3) (1983) 291-299.
[23] J. Du, C. Miao, X. Zhang, I.-H. Jeong, E.M. Son, S. You, B.-J. Lee, D.-K. Kim, Toxicol In Vitro 25(8) (2011) 1535-1541.
[24] K. Zheng, F. Liu, X.-M. Xu, Y.-T. Li, Z.-Y. Wu, C.-W. Yan, New. J. Chem 38(7) (2014) 2964-2978.
[25] A. Lauria, R. Bonsignore, A. Terenzi, A. Spinello, F. Giannici, A. Longo, A.M. Almerico, G. Barone, Dalton Trans 43(16) (2014) 6108-6119.
[26] M. Patel, M. Chhasatia, P. Parmar, Eur. J. Med. Chem 45(2) (2010) 439-446.
[27] B.S. Creaven, M. Devereux, A. Foltyn, S. McClean, G. Rosair, V.R. Thangella, M. Walsh, Polyhedron 29(2) (2010) 813-822.
[28] K. Singh, M.S. Barwa, P. Tyagi, Eur. J. Med. Chem 42(3) (2007) 394-402.
[29] N. Raman, A. Selvan, S. Sudharsan, Spectrochim. Acta. A 79(5) (2011) 873-883.
[30] M.P. Murphy, R.A. Smith, Annu. Rev. Pharmacol. Toxicol. 47 (2007) 629-656.
[31] M. Asadi, Z. Asadi, S.B. Sadi, L. Zarei, F.M. Baigi, Z. Amirghofran, Spectrochim. Acta. A 122 (2014) 118-129.
[32] M. Asadi, S.B. Sadi, Z. Asadi, R. Yousefi, A.R. Barzegar Sadi, H. Khalili-Hezarjaribi, J. Coord. Chem 65(4) (2012) 722-739.
[33] M. Asadi, Z. Asadi, L. Zarei, S.B. Sadi, Z. Amirghofran, Spectrochim. Acta. A 133 (2014) 697-706.
[34] Z. Asadi, M. Asadi, M.R. Shorkaei, J. Iran. Chem. Soc 13(3) (2016) 429-442.
[35] N. Raman, S. Sobha, M. Selvaganapathy, R. Mahalakshmi, Spectrochim. Acta. A 96 (2012) 698-708.
[36] F. Keshavarz, D. Mohammad-Aghaie, Phy. Chem. Res 3(2) (2015) 125-143.
[37] R. Thomsen, M.H. Christensen, J. Med. Chem 49(11) (2006) 3315-3321.
[38] M.A. Lie, R. Thomsen, C.N. Pedersen, B. Schiøtt, M.H. Christensen, J. Chem. Inf. Model 51(4) (2011) 909-917.
[39] A. Satheshkumar, K.P. Elango, Spectrochim. Acta. A 130 (2014) 337-343.
[40] D.M. Boghaei, E. Askarizadeh, A. Bezaatpour, Spectrochim. Acta. A 69(2) (2008) 624-628.
[41] D.X. West, A.A. Nassar, F.A. El-Saied, M.I. Ayad, Trans. Metal Chem 24(6) (1999) 617-621.
[42] M. Tümer, H. Köksal, M.K. Sener, S. Serin, Trans. Metal Chem 24(4) (1999) 414-420.
[43] H.-D. Yin, Q.-B. Wang, S.-C. Xue, J. Organomet. Chem 689(15) (2004) 2480-2485.
[44] J.-P. Cheng, Q.-Y. Lin, H. Rui-Ding, W.-Z. Zhu, H.-Q. Li, D.-H. Wang, Cent. Eur. J. Chem 7(1) (2009) 105-110.
[45] Z.-C. Liu, B.-D. Wang, Z.-Y. Yang, Y. Li, D.-D. Qin, T.-R. Li, Eur. J. Med. Chem 44(11) (2009) 4477-4484.
[46] Z.-C. Liu, B.-D. Wang, B. Li, Q. Wang, Z.-Y. Yang, T.-R. Li, Y. Li, Eur. J. Med. Chem 45(11) (2010) 5353-5361.
[47] P. Krishnamoorthy, P. Sathyadevi, A.H. Cowley, R.R. Butorac, N. Dharmaraj, Eur. J. Med. Chem 46(8) (2011) 3376-3387.

[48] V.M. Manikandamathavan, R.P. Parameswari, T. Weyhermüller, H.R. Vasanthi, B.U. Nair, Eur. J. Med. Chem 46(9) (2011) 4537-4547.
[49] W.J. Mei, J. Liu, K.C. Zheng, L.J. Lin, H. Chao, A.X. Li, F.C. Yun, L.N. Ji, Dalton Trans (7) (2003) 1352-1359.
[50] M. Sirajuddin, S. Ali, A. Badshah, J. Photoch. Photobio. B 124 (2013) 1-19.
[51] S. Sallam, A. Abbas, J. Lumin 136 (2013) 212-220.
[52] H. Wu, J. Yuan, Y. Zhang, F. Shi, G. Pan, J. Kong, X. Fan, Inorg. Chim. Acta 404 (2013) 13-22.
[53] S. Tabassum, S. Amir, F. Arjmand, C. Pettinari, F. Marchetti, N. Masciocchi, G. Lupidi, R. Pettinari, Eur. J. Med. Chem 60 (2013) 216-232.
[54] J. Liu, H. Zhang, C. Chen, H. Deng, T. Lu, L. Ji, Dalton trans (1) (2003) 114-119.
[55] M. Waring, J. Mol. Biol 13(1) (1965) 269-282.
[56] J. Sun, S. Wu, Y. An, J. Liu, F. Gao, L.-N. Ji, Z.-W. Mao, Polyhedron 27(13) (2008) 2845-2850.
[57] S. Sharma, S.K. Singh, M. Chandra, D.S. Pandey, J. Inorg. Biochem 99(2) (2005) 458-466.
[58] X.-L. Wang, H. Chao, H. Li, X.-L. Hong, Y.-J. Liu, L.-F. Tan, L.-N. Ji, J. Inorg. Biochem 98(6) (2004) 1143-1150.
[59] Q.-L. Zhang, J.-G. Liu, J. Liu, G.-Q. Xue, H. Li, J.-Z. Liu, H. Zhou, L.-H. Qu, L.-N. Ji, J. Inorg. Biochem 85(4) (2001) 291-296.
[60] J.M. Kelly, A.B. Tossi, D.J. McConnell, C. OhUigin, Nucleic Acid Res 13(17) (1985) 6017-6034.
[61] J.R. Lakowicz, Principles of fluorescence spectroscopy, Springer Science & Business Media2013.
[62] M.H. Rahman, T. Maruyama, T. Okada, K. Yamasaki, M. Otagiri, Biochem. Pharmacol 46(10) (1993) 1721-1731.
[63] Q. Guo, L. Li, J. Dong, H. Liu, T. Xu, J. Li, Spectrochim. Acta. A 106 (2013) 155-162.
[64] F. Ahmadi, A. Alizadeh, N. Shahabadi, M. Rahimi-Nasrabadi, Spectrochim. Acta. A 79(5) (2011) 1466-1474.
[65] A. Rajendran, C.J. Magesh, P.T. Perumal, Bba-gen. Subjects 1780(2) (2008) 282-288.
[66] X.-Z. Feng, Z. Lin, L.-J. Yang, C. Wang, C.-l. Bai, Talanta 47(5) (1998) 1223-1229.
[67] N. Shahabadi, S. Kashanian, F. Darabi, DNA. Cell. Biol 28(11) (2009) 589-596.
[68] R. Filosa, A. Peduto, S. Di Micco, P. de Caprariis, M. Festa, A. Petrella, G. Capranico, G. Bifulco, Bioorg. Med. Chem 17(1) (2009) 13-24.
[69] J.G. Collins, T.P. Shields, J.K. Barton, J. Am. Chem. Soc 116(22) (1994) 9840-9846.
[70] J.-H. Tan, Y.-j. Lu, Z.-S. Huang, L.-Q. Gu, J.-Y. Wu, Eur. J. Med. Chem 42(9) (2007) 1169-1175.
[71] C. JMDAN, L. Lerman, J. Venable, Nature 236(64) (1972) 67-70.
[72] A.M. Nowicka, A. Kowalczyk, S. Sek, Z. Stojek, Anal. Chem 85(1) (2012) 355-361.
[73] P.U. Maheswari, M. Palaniandavar, J. Inorg. Biochem 98(2) (2004) 219-230.

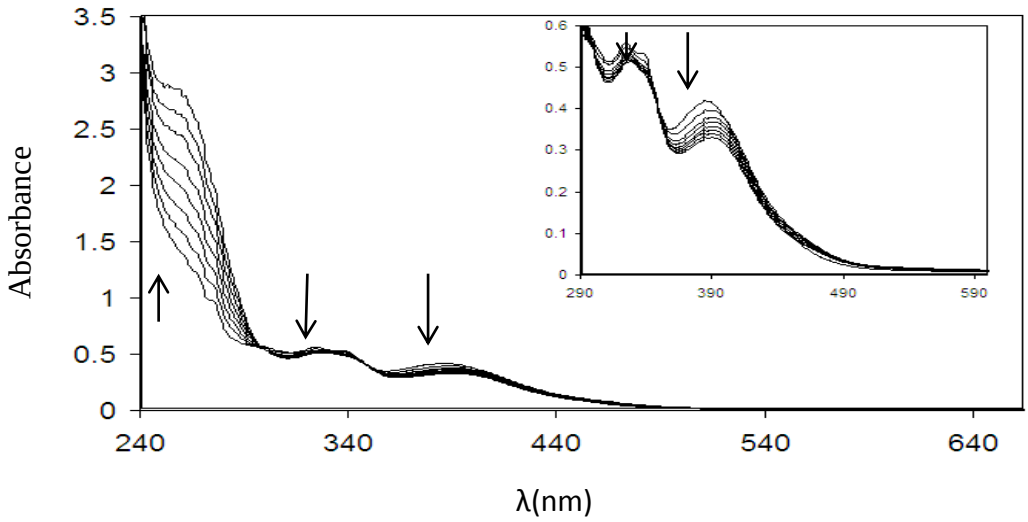

Fig.1. Absorption spectra of complex **2** (50 μM) in 1mM Tris-HCl buffer at pH 7.2, in the absence and presence of increasing amounts of DNA (0-260 μM)

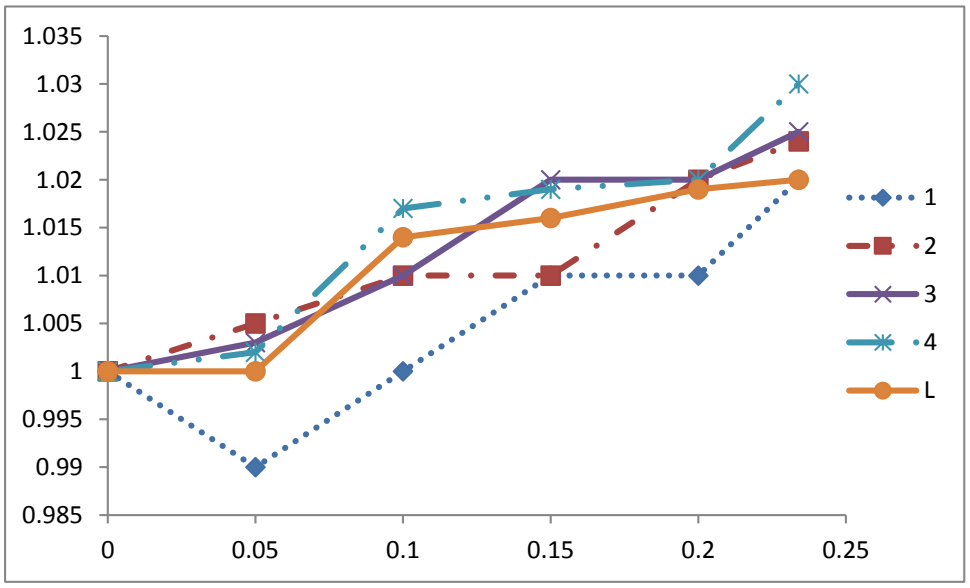

Fig. 2. Effects of increasing amounts of complexes (**1**-**4**)(0-2.34 μM) on the viscosity of DNA(10μM) in 1 mM Tris–HCl buffer. (r = 0.0–0.23) at 25 ℃

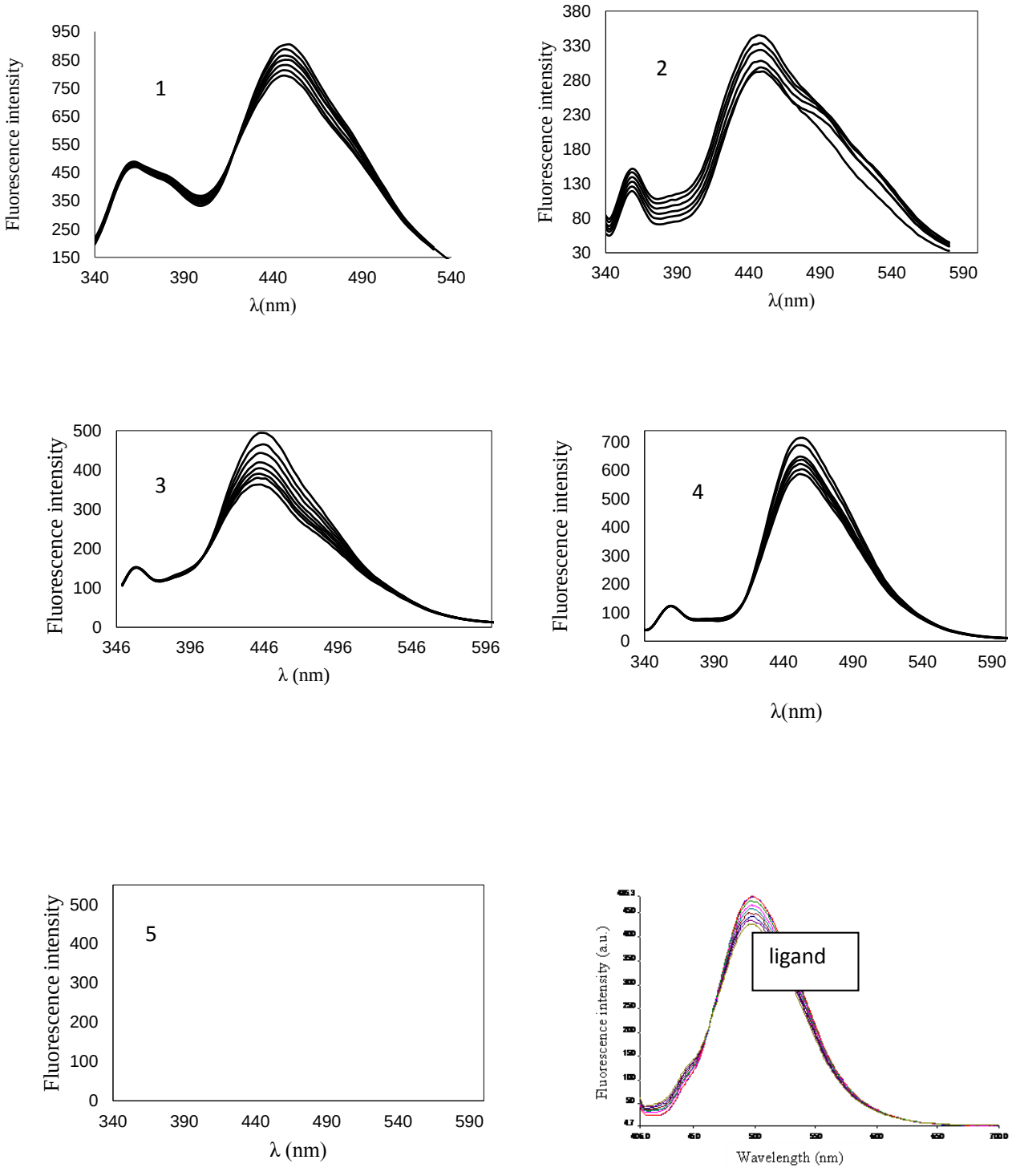

Fig. 3. Effect of F-DNA (in each inject 5 μL 10^{-2} $molL^{-1}$) on the emission intensity of the compound solution

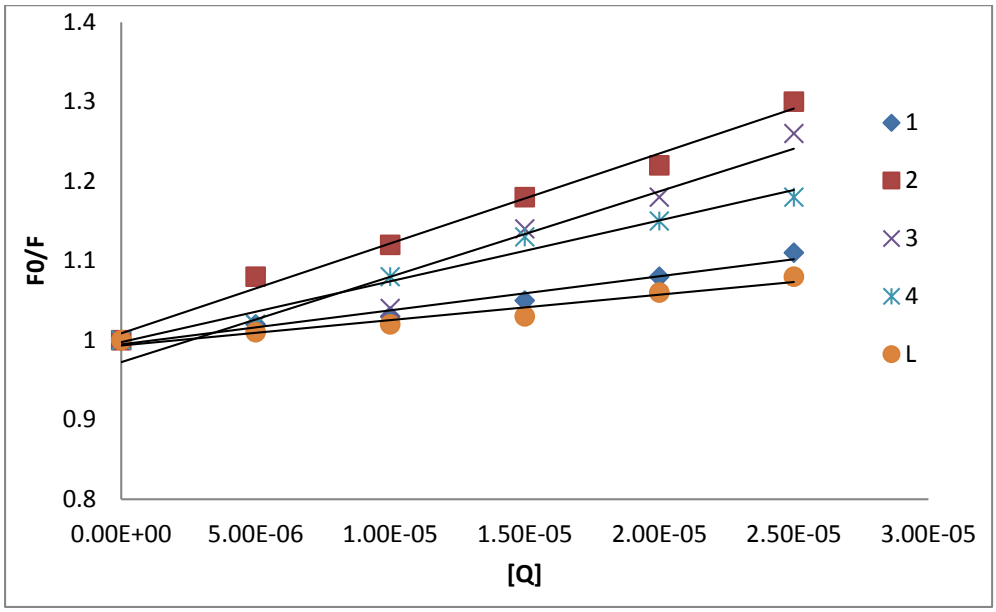

Fig. 4. Stern–Volmer plots for the observed fluorescence of complexes upon addition of DNA.

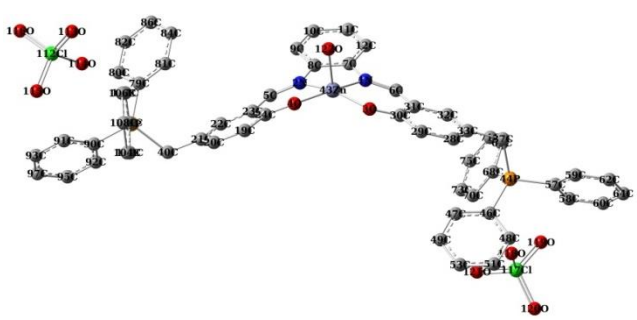

1

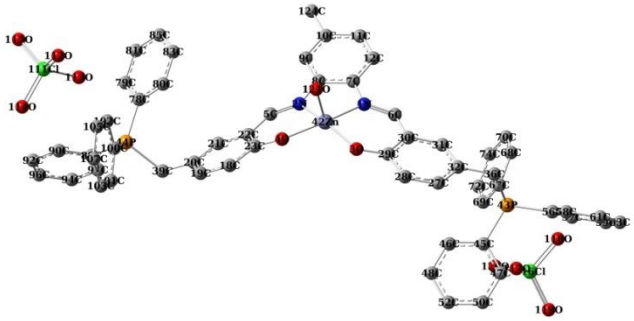

2

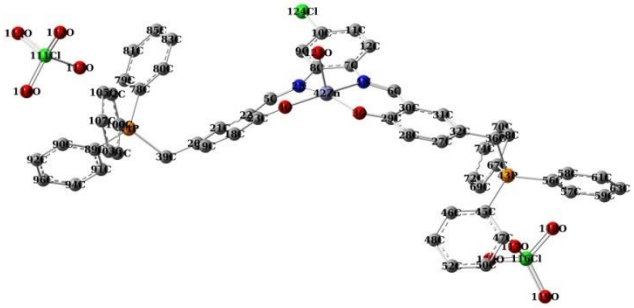

3

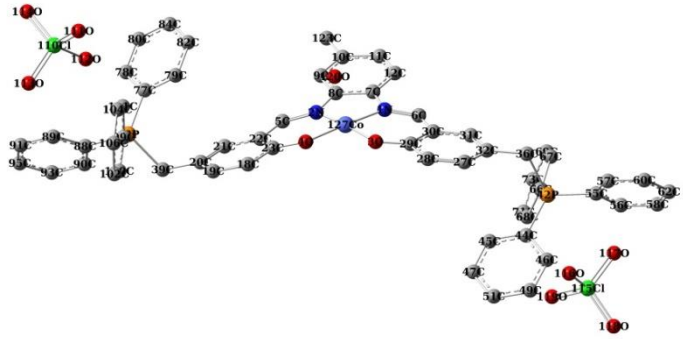

4

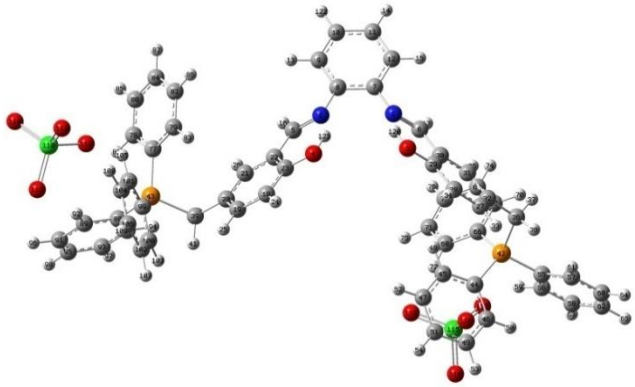

ligand

Fig. 5: The optimized geometrical structure of the complexes and ligand.

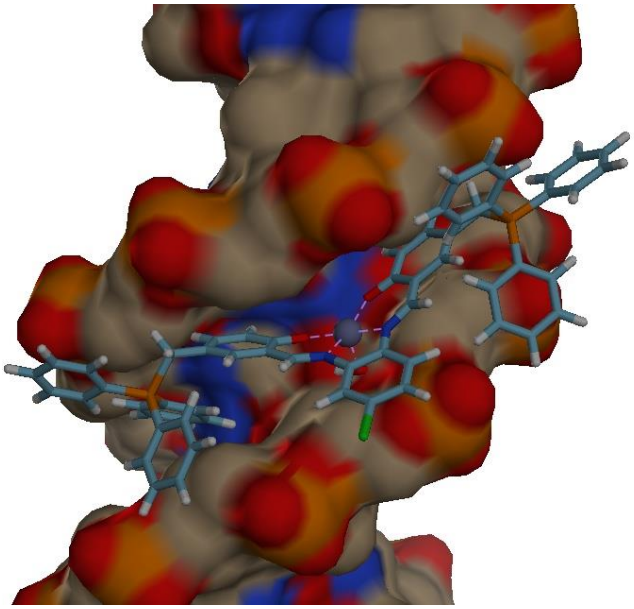

Fig. 6. Computational docking models illustrating the interactions between DNA and complex **4.**

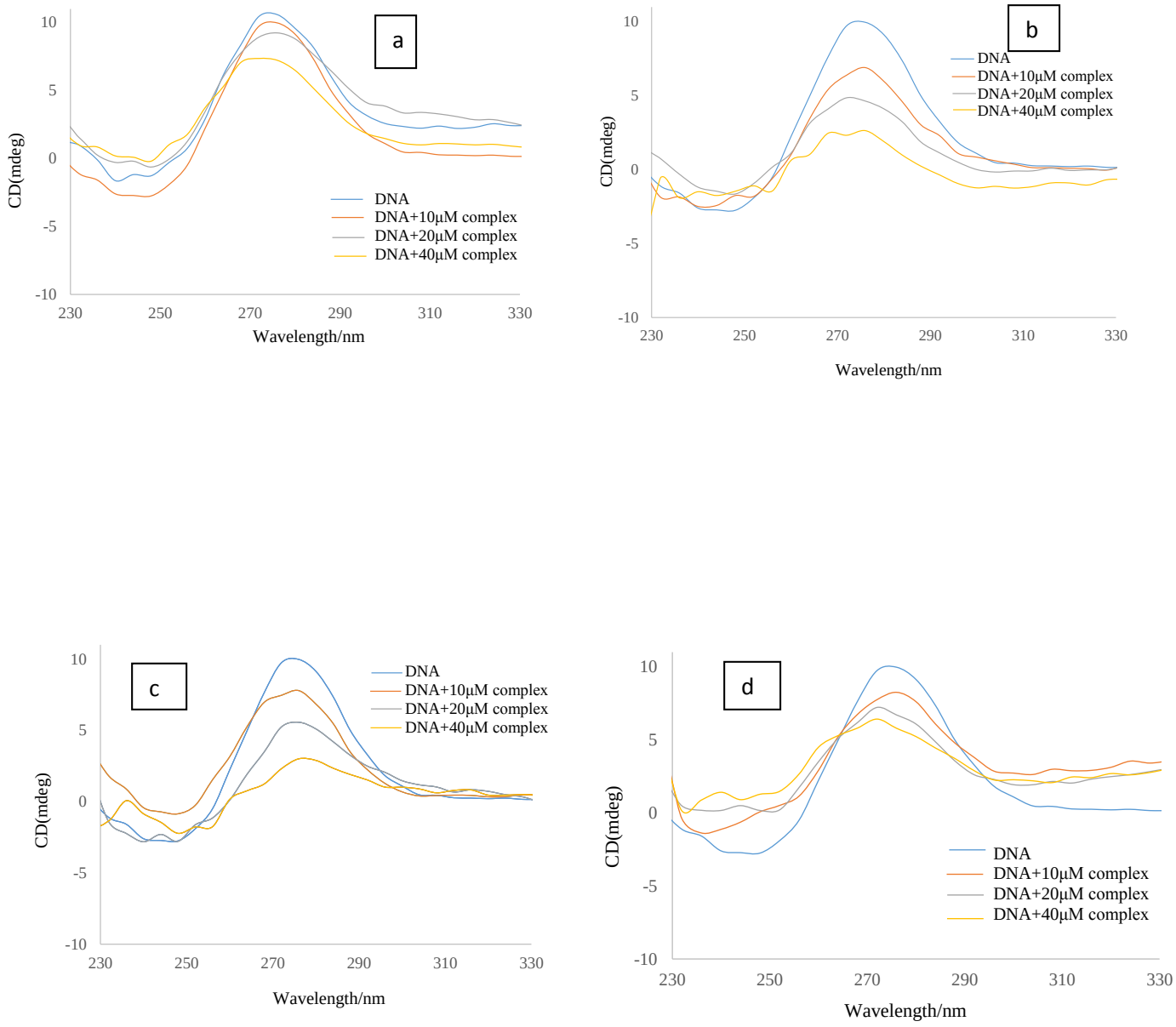

Fig.7. CD spectra of DNA (200 μM) at increasing complex concentration (0- 40 μM) in Buffer (1.0 mM Tris–HCl, 5 mM NaCl); [complex]= 1000 μM, a)complex 1, b) complex 2, c) complex 3, d) complex 4.

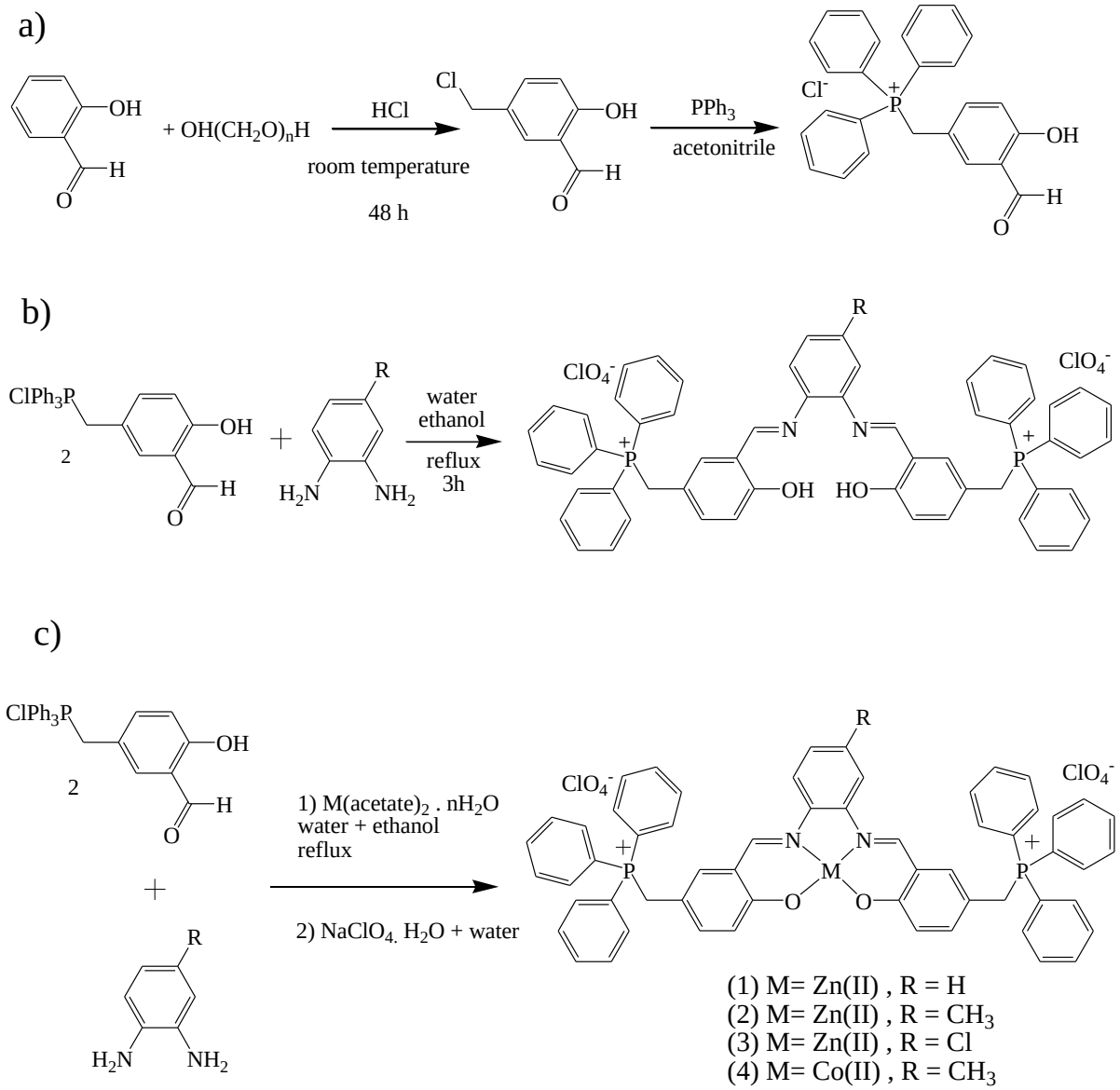

Scheme 1: Synthetic route for a) (3-formyl-4-hydroxybenzyl)triphenylphosphoniumchloride b) ligand c) complexes **1-4**.

Table 1: Absorption spectral properties of compounds bound to DNA

Compound	λ (nm)	Change in absorbance	$K_b(M^{-1})$
L	384	Hypochromism	1.22×10^{1}
1	360	Hypochromism	2.54×10^{2}
2	320	Hypochromism	1.05×10^{4}
3	385	Hypochromism	5.13×10^{3}
4	420	Hypochromism	1.15×10^{3}

Table 2: The Stern-Volmer quenching constant for the interaction of complexes with DNA.

complex	K_{sv} (M^{-1})	k_q ($M^{-1}s^{-1}$)
L	1124	1.1×10^{11}
1	4285	4.2×10^{11}
2	11314	11.3×10^{11}
3	10743	10.7×10^{11}
4	7657	7.6×10^{11}

Table 3. The inhibitory concentration (IC_{50}) for the effects of the complexes on various cell lines

compounds	IC_{50} (μg/ml)		
	A549	Jurkat	Raji
1	26.7±1.3	19.5±0.6	16.2±1.3
2	13.6±0.6	8.7±0.4	10.2±1.6
3	21.2±0.9	16.2±0.5	10.8±0.7
4	18.6±0.4	22.4±1.4	20.5±2.4
cis-platin	79.4±1.3	25.0±1.4	30.1±0.7

Table 4. Selected bond lengths in Aº and angles (º) by theoretical calculation at B3LYP method.

Bond length				
complex	**1**	**2**	**3**	**4**
M-N_1	2.0818	2.0816	2.0844	1.9091
M-N_2	2.0832	2.0820	2.0851	1.9116
M-O_3	1.9685	1.9668	1.9649	1.9014
M-O_4	2.0067	2.0102	2.006	1.9148
M-O(H_2O)	2.1048	2.1055	2.0994	2.2172
Bond angle				
complex	**1**	**2**	**3**	**4**
N_1-M-N_2	79.54370	79.66400	79.47104	85.40602
N_1-M-O_3	89.16654	89.38283	89.23447	93.50707
N_2-M-O_4	87.57768	87.49896	87.36105	93.27829
N_1-M-O_4	165.49812	166.12785	165.80639	176.72227
N_2-M-O_3	159.27143	158.30187	157.87078	173.47574
O_3-M-O_4	100.98148	100.97247	101.36446	87.46189

Table 5. Docking results for binding score of the ligand and complexes to the DNA structure.

Pose	Rerank Score				
	Complex 2	**Complex 1**	**Complex 3**	**Complex 4**	**Ligand**
1	**-114.267**	-99.5206	**-102.659**	**-102.189**	**-96.953**
2	-94.3518	**-100.261**	-82.0867	-100.398	-93.074
3	-87.0785	-97.2592	-80.0382	-93.6988	-90.354
4	-80.2376	-97.7859	-79.3021	-92.9935	-87.397
5	-75.1788	-85.3717	-82.2511	-86.3833	-83.606
6	-75.1764	-78.9442	-77.4199	-90.1663	-96.953
7	-74.5466	-82.1819	-80.4708	-85.1204	-93.074
8	-68.6455	-77.356	-77.4585	-84.754	-90.354
9	-71.7893	-79.5016	-71.9243	-79.3141	-87.397
10	-74.0445	-78.2983	-68.4455	-80.6355	-83.606